



CHEMICAL AND STRUCTURAL CHARACTERIZATION OF SLAG COMPOUNDS FORMED IN THE MELTING PROCESSES TO PRODUCE SPHEROIDAL GRAPHITE CAST IRONS

Anna Regordosa 

Departament de Metal·lúrgia, Fundería Condals, S.A, 08241 Manresa, Spain

Departament de Ciència dels Materials I Enginyeria Metal·lúrgica, Universitat de Barcelona, 08028 Barcelona, Spain

Núria Llorca-Isern

Departament de Ciència dels Materials I Enginyeria Metal·lúrgica, Universitat de Barcelona, 08028 Barcelona, Spain

Copyright © 2016 American Foundry Society

DOI 10.1007/s40962-016-0025-7

Abstract

The aim of this research is to investigate the composition and phases present in the slags formed during the production of spheroidal graphite cast irons. This paper contains the results of the first part of such investigation which is focused on those slags generated in the induction furnace, i.e., solid slags formed on the melt surface and slags adhered to quartzite refractory lining. Thus, a group of slag samples of each type were obtained from melts prepared using different metallic charges. These samples were then characterized in order to determine their chemical and structural composition and to evaluate the influence of the raw materials used during melting process on the amount of slag formed in each case. Three different techniques were used for analyzing the slag samples: X-ray fluorescence, X-ray diffraction and scanning electron microscopy with EDS microanalysis. Important differences have been detected among samples studied in this work that have revealed the detrimental role of aluminum on refractory linings. The obtained knowledge has been successfully used to minimize the problems caused by adhesion of slags to refractory linings.

Keywords: spheroidal graphite cast irons, slag compounds, induction furnace, refractory lining, X-ray diffraction, X-ray fluorescence, scanning electron microscopy

Introduction

One of the main problems of spheroidal graphite (SG) cast iron production is the formation of slag compounds that can be formed in any of the various stages of the manufacturing process. The consequence of the formation of these slag compounds depends on the stage in which they are formed. Slag inclusions can be found as an inclusion in the manufactured parts, which is one of the most common defects,^{1,2} but they can also be found, as adhered products in the refractory linings of melting furnaces. In this second case, important reductions on the internal diameter of refractory crucibles are detected which decrease the effective capacity of melting furnaces. In addition to this fact, the formation of such slag accumulations causes cracks and erosion in the silica refractory lining and it promotes failures on the inductor isolation systems.^{3,4} The other important source of active slag is the treatment of base melts with magnesium ferroalloys.⁵ These slag

compounds have to be properly removed from ladles in order to minimize subsequent contamination problems on pouring devices used in foundry plants. Otherwise such slag products will be rapidly deposited on the refractory lining, and a high risk of degradation will be present in the pouring tools. In general, filters and/or proper filling systems are commonly used in molds for avoiding the appearance of slag inclusions on castings.

In order to avoid the problems related to the formation of slag, it is important to know its chemical composition and those phases present in the slag compound formed at different stages of the production process of SG cast irons. This information becomes useful to determine the affecting chemical elements and which of them are present in the different types of slag commonly found in SG cast iron manufacture. Previous studies⁶ on slag formed in spheroidal and lamellar cast irons have shown that it mostly consists of several oxides as FeO, MnO, SiO₂, Al₂O₃ and

81 MgO. It has been also reported that these oxides except
 82 FeO and MnO are solid in the melting temperature range.
 83 According to the Ellingham's diagram, the formation of
 84 these oxides is the result of a balance between the oxida-
 85 tion of such elements and the oxidation of carbon for a
 86 given temperature. In accordance with the mentioned
 87 literature data, there is a temperature range around
 88 1427 °C (2600 °F)–1482 °C (2700 °F) in which slag
 89 formation and the appearance of CO gas by carbon oxida-
 90 tion on melts are minimal. These authors observed an
 91 increase on slag formation temperature when increasing
 92 the silicon content for a given carbon content in the melt.
 93 The contrary effect was also detected. It is also reported
 94 that re-oxidation reactions occur when free-slag melts
 95 cool down, so liquid and solid slag compounds can be
 96 formed again due to the oxidation of alloying elements
 97 present in the liquid cast iron.

98 In a more recent work⁷, the influence of metallic charge
 99 contents on the amount of slag formed and on its chemical
 100 composition was studied though any information about the
 101 phases involved was not reported. These authors found the
 102 lowest amount of slag after melting when high purity pig
 103 iron was used as the main constituent of metallic charges.
 104 The worst result (highest amount of slag) was found when
 105 using foundry returns composed by shot-blasted ferritic
 106 ductile iron casting scrap, while intermediate results were
 107 obtained when using steel scrap according to its composi-
 108 tion and its source. It was also concluded that the composi-
 109 tion of the formed slag depends on the metallic charge
 110 type. All metallic charge compositions originated a slag
 111 type with similar SiO₂ and Al₂O₃ contents (both were the
 112 main oxides) which was obtained from the refractory lining.
 113 Slag found when using HPI and steel scrap metallic
 114 charges shows relevant amounts of CaO, while MnO was
 115 found on slag obtained from metallic charges that mainly
 116 contained foundry returns and steel scrap. Finally, slag
 117 formed after melting ductile iron returns showed important
 118 MgO contents. Surprisingly, any contribution on slag
 119 composition of silicon content in alloys and of the raw
 120 materials cleanliness (this second parameter mainly affected
 121 by external oxidation of pig iron) was not found in that
 122 mentioned work.⁷

123 Katz⁸ showed the harmful effects of Fe–O-bearing slag
 124 which promote the oxidation of valuable elements such as
 125 C and Mn. On the other hand, this slag also sticks on the
 126 silica refractory which is the most commonly used in
 127 electric furnaces. Additions of SiC in the melting furnace
 128 are recommended in this work to avoid this problem. It also
 129 reported that such slag sources were sand residues present
 130 in the foundry returns and oxidized compounds normally
 131 found on raw materials surfaces in case of melting processes
 132 made with electric furnaces.

133 Considering the results of previous studies, two different
 134 aims have been approached in this work: the study of the

chemical composition changes and of the different com- 135
 pounds found in slag samples depending on the raw 136
 materials used for preparing melts and the minimization of 137
 detrimental effects caused by slag which is stuck to the 138
 refractory linings. 139

Experimental Work 140

In a first step, six different base melts were prepared in a 6-t 141
 capacity medium frequency induction furnace (250 Hz, 142
 4250 kW) using three different metallic charge composi- 143
 tions and two maximum temperatures (see Table 1). In all 144
 cases, these raw materials were introduced in the furnace 145
 crucible when a remaining amount of melt (around 4000 kg) 146
 was present in it. The composition of each remaining melt 147
 was the one that corresponds to a standard metallic charge 148
 previously melted in the furnace (see Table 2). Note that 149
 the FeSi alloy was only used with pig iron and steel scrap-based 150
 charges, while graphite and SiC were exclusively used for 151
 preparing the melts with steel scrap. After melting and just 152
 after achieving the maximum temperature, an alloy sample 153
 and a slag sample were simultaneously extracted from each 154
 base melt surface. Then, a second sampling was made after 155
 skimming the surface of melts and then remaining them in 156
 contact with open air for 45 min at each of the two selected 157
 maximum temperatures. The first and the second groups of 158
 samples will be identified as initial (I) samples and as final 159
 (F) samples, respectively. These samples have been also 160
 identified according to the metallic charge composition (PI 161
 for pig iron, FR for foundry returns and SC for steel scrap) 162
 and to the maximum temperature achieved during melting 163
 process (00 for 1500 °C (2732 °F) and 45 for 1545 °C 164
 (2813 °F), see Table 1). For instance, the PI00I code is used 165
 to identify the samples that have been initially picked up 166
 from the base melt prepared with pig iron at 1500 °C 167
 (2732 °F). 168

In a second step, three slag samples adhered to different 169
 refractory linings of the induction furnace have been 170
 studied. These samples were removed from the refractory 171
 surface at the end of the life span of the furnace linings 172
 which duration was not systematically the expected one 173
 due to failures on the inductor isolation system. In these 174
 cases, the metallic charge composition was commonly used 175
 in the manufacturing process of the foundry plant (Table 2) 176
 and the melting procedure was similar to the one detailed 177
 above. These samples will be identified in the text as 178
 UC11, UC31 and UC32 where UC notation refers to “usual 179
 charges,” the first number is the furnace identification and 180
 the second one is the sample number. 181

In a third step of the present work, a set of experiments 182
 were made in order to obtain more information about the 183
 formation of slags stuck to the refractory linings. Thus, two 184
 different metallic charges, one based on foundry returns 185
 and the other one based on steel scrap, were exclusively 186

Table 1. Temperatures of Melts Prepared in the Induction Furnace and Metallic Charge Compositions (kg)

| Sample | T/°C (°F) | Pig iron | Steel scrap | Returns | Graphite ^a | FeSi ^b | SiC ^c |
|-------------|-------------|----------|-------------|---------|-----------------------|-------------------|------------------|
| PI00I/PI00F | 1500 (2732) | 1923 | – | – | – | 31 | – |
| FR00I/FR00F | 1500 (2732) | – | – | 1838 | – | – | – |
| SC00I/SC00F | 1500 (2732) | – | 1866 | – | 75 | 29 | 19 |
| PI45I/PI45F | 1545 (2813) | 1966 | – | – | – | 41 | – |
| FR45I/FR45F | 1545 (2813) | – | – | 1890 | – | – | – |
| SC45I/SC45F | 1545 (2813) | – | 1838 | – | 67 | 24 | 19 |

^a Carbon content: 99.9 wt%

^b FeSi composition: 75.2 wt% Si, 0.7 wt% Al and 0.3 wt% Ca

^c SiC composition: 65 wt% Si, 25 wt% C and 0.8 wt% Al

Table 2. Metallic Charge Compositions Used in the Induction Furnace (wt%)

| Sample | Pig iron | Steel scrap | Returns | Graphite ^a | FeSi ^b | SiC ^c |
|-------------------|----------|-------------|---------|-----------------------|-------------------|------------------|
| FR21 | 2.6 | 30 | 65 | 1.2 | 0.2 | 0.5 |
| SC31 | 3.0 | 65 | 28 | 2.6 | 1.0 | 0.7 |
| Usual charge (UC) | 2.5 | 37 | 59 | 1.4 | – | 1.0 |

^a Carbon content: 99.9 wt%

^b FeSi composition: 75.2 wt% Si, 0.7 wt% Al and 0.3 wt% Ca

^c SiC composition: 65 wt% Si, 25 wt% C and 0.8 wt% Al

187 used for preparing all the base melt batches during the
 188 whole life span of each refractory lining in the furnace.
 189 Table 2 shows the composition of these two metallic
 190 charges which were introduced in the furnace with around
 191 4000 kg of remaining melt except in the first charge where
 192 the furnace was empty. In all cases, the maximum temper-
 193 ature achieved during the melting process was 1500 °C
 194 (2732 °F). After finishing the life span of these two
 195 refractory linings, a slag sample was obtained from each
 196 one for later characterization. These two slag samples are
 197 identified as FR21 and SC31 where FR and SC notations
 198 refer to foundry returns or to the steel scrap-based charges,
 199 respectively. The first number is the furnace identification,
 200 and the second one is the sample number.

201 Chemical compositions of melts were determined on
 202 samples picked up from the prepared alloys during slag
 203 sampling. These analyses were performed using a combus-
 204 tion technique (LECO CS200) for carbon and sulfur and
 205 spark emission spectroscopy (ARL Metal Analyzer
 206 Iron + Steel) for the rest of elements.

207 X-ray fluorescence (XRF), X-ray diffraction analysis
 208 (XRD) and scanning electron microscopy (SEM) and EDS
 209 microanalysis were used for characterizing the slag sam-
 210 ples. The first technique was used to determine chemical
 211 compositions of slag. Thus, samples were crushed and then
 212 were burned at 950 °C (1742 °F) for 24 h to remove any
 213 remaining amount of carbon and/or sulfur. Then, 0.15 g of
 214 calcined sample was mixed with 5.7 g of lithium

tetraborate (1/40 dilution) and 5 mg of lithium iodide as
 215 surfactant factor was finally added to the mixture. This
 216 mixture was melted at 1100 °C (2012 °F) in an induction
 217 furnace (Perle'X-3) to obtain the 30 mm (1.18 inches) in
 218 diameter pearls for XRF analysis. The fluorescence intensi-
 219 ty was measured with a AXIOS Advanced wavelength
 220 dispersion X-ray sequential spectrophotometer equipped
 221 with a semiquantitative software program for elements
 222 with atomic number higher than 9 (F), using as excitation
 223 source a tube with a Rh anode. The quantification of the
 224 elements is done using a calibration line previously made
 225 with international reference geological samples pearl (di-
 226 lution 1/40) to analyze their chemical composition by XRF.
 227

XRD was used to characterize the constituent phases
 228 formed on each slag sample by means of a PANalytical
 229 X'Pert PRO MPD q/q Bragg–Brentano powder diffrac-
 230 tometer 240 mm (9.45 inches) in radius. The slag samples
 231 were crushed in an agate mortar until micrometer size.
 232 Then, the sample was placed in a rectangular standard
 233 holder 20 mm (0.79 inches) in length, 15 mm (0.59 inches)
 234 in width and 1 mm (0.04 inches) in height in order to
 235 obtain a flat surface by manual pressing of the powder
 236 material using a glass plate.
 237

Scanning electron microscopy and EDS microanalysis
 238 (SEM–EDS) were used to corroborate the results obtained
 239 from the two other techniques and to check the slag sam-
 240 ples' microstructure. For this purpose, the raw samples
 241 were broken in small pieces and then were embedded in
 242

243 epoxy resin at room temperature. After conditioning the
 244 embedded samples for metallographic inspection, they
 245 were sputtered with carbon and then analyzed using a
 246 ESEM Quanta 200 FEI, XTE 325/D8395 with observa-
 247 tion conditions of AV = 20.00 kV, WD = 10 mm
 248 (0.39 inches) and intensity probe of 4.5 nA. Secondary
 249 electron mode (SE Image) and backscattered electron mode
 250 (BSE Image) were also used for characterizing the slag
 251 samples.

252 Results and Discussion

253 Slags Generated in Induction Furnaces

254 After melting the metallic charge and then stopping the
 255 induction power in the furnace, the slag formed is normally
 256 found as scabs which are floating in the melt surface. These
 257 slags are formed in the melt surface areas that are close to
 258 the refractory lining, but then they become aggregated in a
 259 crust form found in the central area. Once extracted from
 260 the melt and then cooled at room temperature, the slag
 261 shows an apparent vitreous morphology and a dark gray
 262 color. A second inspection of melts surfaces after skim-
 263 ming process shows that more slags were gradually formed
 264 in the surface of melts. Color and morphology of these
 265 recent slag compounds are similar to the ones initially
 266 obtained. The chemical composition ranges of the prepared
 267 melts are shown in Table 3. It is noted that the alloy
 268 obtained when using the steel scrap-based charge shows
 269 aluminum, manganese and zinc contents that are signifi-
 270 cantly higher than the two others. On the other hand, alu-
 271 minum has been also added by means of SiC and FeSi
 272 products that were used for adjusting the melt composition
 273 in these cases (Table 1). However, the last product does not
 274 seem to be very relevant in this sense as aluminum contents
 275 are higher for alloys prepared with charges based on
 276 returns than for those prepared using pig iron as main raw
 277 material (Table 3). On the other hand, the use of returns
 278 seems to be the cause of the highest silicon contents
 279 observed on the base alloys investigated. The highest sulfur
 280 levels are found when using pig iron-based charges due to
 281 the high content of this element commonly found in this
 282 raw material.

283 The results obtained from the XRF analyses performed on
 284 the twelve slag samples collected from base irons can be
 285 seen in Table 4. In this table, only those values higher than
 286 1.00 wt% are shown. The results indicate that silicon oxide
 287 is the main constituent of all these samples. Thus, SiO₂ is
 288 shown to be the most important oxidation product in melts
 289 as silicon is the main alloying element and this element
 290 exhibits a high tendency to be oxidized. As can be
 291 expected, the four slag samples obtained from the melt
 292 prepared using foundry returns show the highest SiO₂
 293 contents (Table 4) due to the sand adhered to these raw
 294 materials and owing to the high silicon content found on
 295 the corresponding base melts (see Table 3). The SiO₂
 296 content is also higher in the slag samples extracted after
 297 45 min than in those collected just after melting. This
 298 result could be related to the progressive oxidation of sil-
 299 icon while keeping melts in the furnace at a given tem-
 300 perature. However, a similar effect due to the use of high
 301 temperatures has not been detected.

302 The aluminum oxide content in the slag samples obtained
 303 from the two steel scrap-based melts is higher than the ones
 304 extracted from the pig iron-based melts. Although the exclu-
 305 sive SiC addition made when preparing the steel scrap-based
 306 melt can be related to this fact, another important available
 307 source of aluminum can be the own steel scrap. The Al₂O₃
 308 content is also higher in the samples obtained from melts that
 309 were remaining in the furnace than the ones obtained just after
 310 melting the metallic charges. This is probably due to the
 311 progressive oxidation of aluminum present in the liquid alloy
 312 during the remaining time. The high CaO levels found in the
 313 slag samples collected from the melts prepared using steel
 314 scraps and pig iron can be explained by the addition of the FeSi
 315 ferroalloy. Clear tendencies when comparing the chemical
 316 compositions of the slag samples obtained at 1500 °C
 317 (2732 °F) or at 1545 °C (2813 °F) are not observed.

318 The XRD analyses carried out on all the slag samples
 319 studied in the present work support the results obtained by
 320 XRF. Floating slags generated in the induction furnace are
 321 mainly composed by amorphous phases. The two main
 322 phases with crystalline structures that have been found on
 323 these samples are quartz and cristobalite (SiO₂). Quartz is
 324 the stable phase at temperatures lower than 867 °C

Table 3. Chemical Compositions of the Base Melts Prepared in the Present Work (wt%)

| Samples | C | Mn | Si | S | Mg | Al | Ti | Ce | Zn |
|-------------|------|------|------|-------|-------|--------|-------|--------|-------|
| PI00I/PI00F | 3.90 | 0.18 | 2.02 | 0.020 | 0.002 | 0.0020 | 0.024 | 0.0018 | 0.079 |
| FR00I/FR00F | 3.83 | 0.22 | 2.12 | 0.011 | 0.003 | 0.0029 | 0.023 | 0.0019 | 0.081 |
| SC00I/SC00F | 3.79 | 0.29 | 1.97 | 0.014 | 0.002 | 0.0091 | 0.021 | 0.0024 | 0.199 |
| PI45I/PI45F | 3.98 | 0.18 | 1.78 | 0.021 | 0.002 | 0.0021 | 0.021 | 0.0021 | 0.091 |
| FR45I/FR45F | 3.85 | 0.20 | 1.98 | 0.014 | 0.003 | 0.0029 | 0.024 | 0.0024 | 0.107 |
| SC45I/SC45F | 3.76 | 0.21 | 1.82 | 0.014 | 0.003 | 0.0066 | 0.031 | 0.0023 | 0.218 |

Table 4. Chemical Composition of Floating Slag Samples Analyzed by XRF (wt%)

| Samples | SiO ₂ | Al ₂ O ₃ | MgO | CaO | Fe ₂ O ₃ | MnO | ZnO | CeO ₂ |
|---------|------------------|--------------------------------|-------|-------|--------------------------------|------|------|------------------|
| PI00I | 56.90 | 5.83 | 2.51 | 7.31 | 20.26 | 3.27 | – | – |
| PI00F | 63.21 | 10.16 | 3.45 | 6.29 | 3.70 | 2.38 | – | – |
| FR00I | 59.40 | 4.68 | 3.92 | 2.73 | 21.11 | 4.12 | 1.55 | – |
| FR00F | 76.60 | 7.26 | 5.16 | 3.11 | 1.22 | 1.24 | – | – |
| SC00I | 50.99 | 6.59 | 3.95 | 3.10 | 8.53 | 2.47 | 1.43 | – |
| SC00F | 61.37 | 18.72 | 5.72 | 4.34 | 2.46 | 1.80 | 1.45 | – |
| PI45I | 64.14 | 6.33 | 1.97 | 12.83 | 7.08 | 4.66 | – | – |
| PI45F | 62.46 | 10.31 | 3.34 | 8.16 | 8.17 | 2.02 | 1.07 | – |
| FR45I | 69.90 | 8.02 | 10.54 | 3.36 | 1.19 | 1.56 | – | 1.88 |
| FR45F | 68.72 | 8.17 | 9.58 | 3.74 | 2.04 | 1.21 | – | 1.68 |
| SC45I | 41.59 | 9.59 | 10.51 | 12.86 | 9.15 | 1.15 | – | 1.01 |
| SC45F | 56.74 | 21.65 | 7.07 | 4.32 | 3.05 | 1.91 | 1.89 | 1.27 |

(1593 °F), tridymite is the stable phase from 867 °C (1593 °F) to 1470 °C (2678 °F), while cristobalite is the stable phase at higher temperatures above this value. The tridymite phase is not present in the slag samples studied in the present work because is more frequent the crystallization of the cristobalite than the tridymite due to the absence of the tridymite stabilizer oxides.⁹

The other oxides detected in the XRF analyses but not found as crystalline phases by XRD are contained in the mentioned amorphous part of the slag. Two micrographs included in Figure 1 show how the SiO₂ crystals grow in the amorphous matrix of the FR45I and FR45F slag samples. The SEM observation of these crystalline phases shows dendritic-type morphologies typically found on phases that nucleate and grow from the liquid alloy.

In addition to the main SiO₂ phases, minor amounts of some silicates and other oxides have been also detected in five of the slag samples analyzed by XRD. Magnesium silicates are found in two of the slag samples obtained from base melts prepared with foundry returns (FR00I and FR45F). In the sample FR45F, a magnesium iron oxide (MgFe₂O₄) is also found. The presence of these Mg-bearing slag compounds in such samples is related to the use of ductile iron returns as raw materials when preparing the base melts mentioned above. On the other hand, crystalline iron silicate ((Fe,Ca)₂(SiO₃)₂) and iron oxide (Fe₂O₃) are, respectively, detected on PI00I and PI45F samples, while zinc silicate (Zn₂SiO₄) is present in the SC45F sample. In this last, zinc oxide (ZnO) and an aluminum zinc oxide (ZnAl₂O₄) are found too. As expected, the iron silicate is found in a sample obtained from a melt prepared with pig iron (surface oxidation), while the zinc compounds are only detected when galvanized steel scrap is used as raw material during melting. Figure 2 shows the XRD spectrum and indexation of the three crystalline phases found in the FR00I slag sample, i.e., quartz, cristobalite and pigeonite

(Mg,Ca,Fe)SiO₃. On the other hand, Figure 3 illustrates the crystalline growth of a silicate-type compound (a) found in the same sample and the results obtained from the SEM-EDS microanalysis (b) of such compound.

Besides, some nondissolved particles of SiC and/or FeSi were detected by XRD on samples obtained from melts prepared using these additives (see Table 1). Subsequent SEM analyses made on such samples confirmed these results.

As it has been stated before, the zinc content both in the prepared melts and in the slag samples extracted after melting becomes high when the steel scrap-based metallic charges are used as the galvanized steel scrap from the automotive industry is the main constituent of these charges. This fact is confirmed by means of the XRD analysis made on the slag samples. Figure 4 shows the XRD diffractogram recorded on the SC45F slag sample where the minor crystalline phases are very easily identifiable even though a high content of amorphous phases is found in this sample. Thus, peaks of Zn₂SiO₄ (willemite) and ZnO are detected in addition to the ones that belong to ZnAl₂O₄ (gahnite), the latter only appearing in this slag sample. Although all these zinc-bearing phases have not been detected by SEM analysis because they are present in a very minor amount, the microanalysis made on the amorphous phase of the SC45F slag sample shows a small peak of zinc (this sample contains the highest ZnO and Al₂O₃ contents of all samples analyzed) (see Table 4).

Slags Adhered to the Refractory Lining of Induction Furnaces

Characterization of Slags (Standard Metallic Charges)

After emptying and then cooling, the furnace crucible slags adhered to the refractory lining are detected in an area located close to the bottom of the crucible and at 1/3 of its

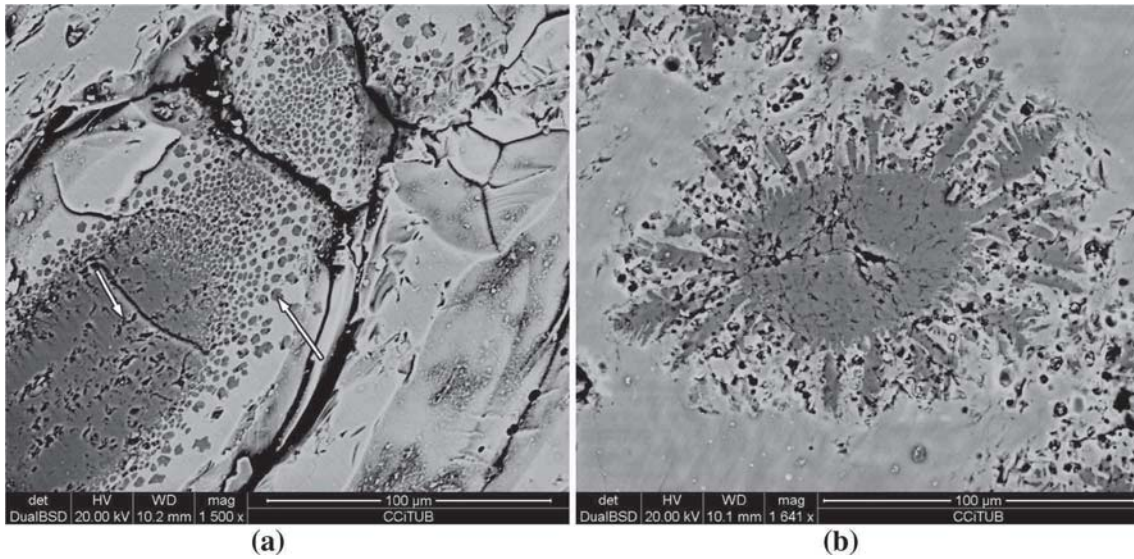


Figure 1. The SiO_2 crystalline phase growing in the amorphous matrix of the FR45I (a) and the FR45F (b) slag samples.

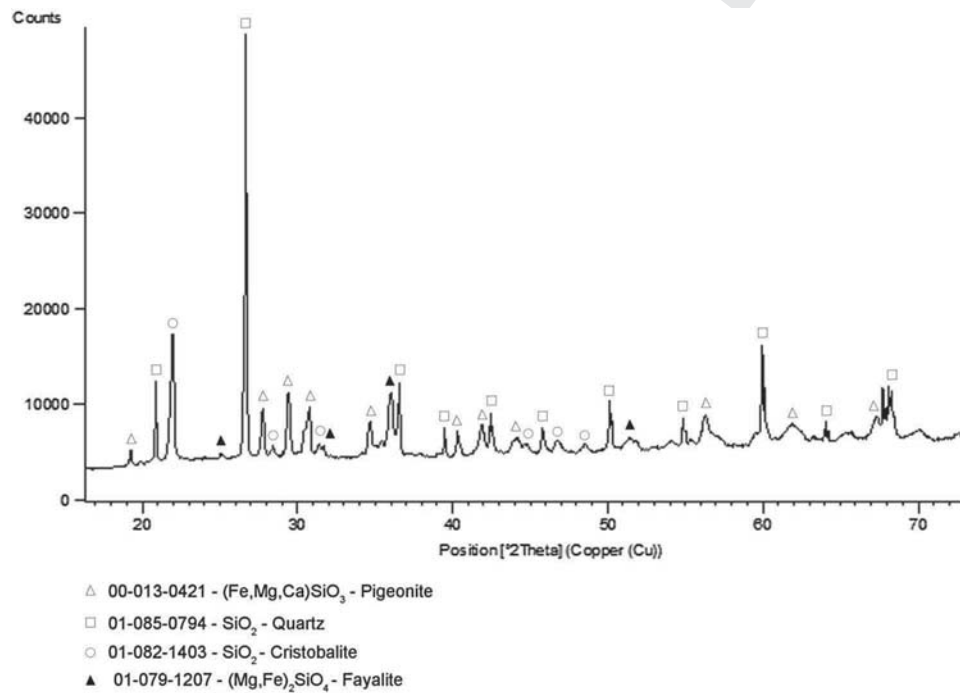


Figure 2. XRD diffractogram and phases indexation on the FR00I sample: quartz, cristobalite and pigeonite $[(\text{Mg},\text{Ca},\text{Fe})\text{SiO}_3]$ were found.

394 total height. This affected area always remains in contact
 395 with the liquid alloy even after tapping the furnace
 396 according to the usual procedure of the plant. The thickness
 397 of the slags found in this affected area ranges from 20 mm
 398 (0.79 inches) to 150 mm (5.91 inches), and they seem to be
 399 heavier than those floating slags directly obtained from
 400 melts. Figure 5 shows a general view of a discharged
 401 refractory lining of a furnace. The zone marked as 1 in this
 402 figure is the worn part of the refractory lining. Notice that

the expected thickness of the used refractory lining can be 403
 found in the upper levels (marked in Figure 5 with arrows). 404
 The adhered slags were found below zone 1, and they 405
 affect the whole section of the lining at this lower level 406
 (zone 2 in Figure 5). 407

Quartzite refractory areas in contact with slag showed a 408
 darker region with around 1 cm in thickness which is 409
 marked by arrows in Figure 6a. A general view of a slag 410

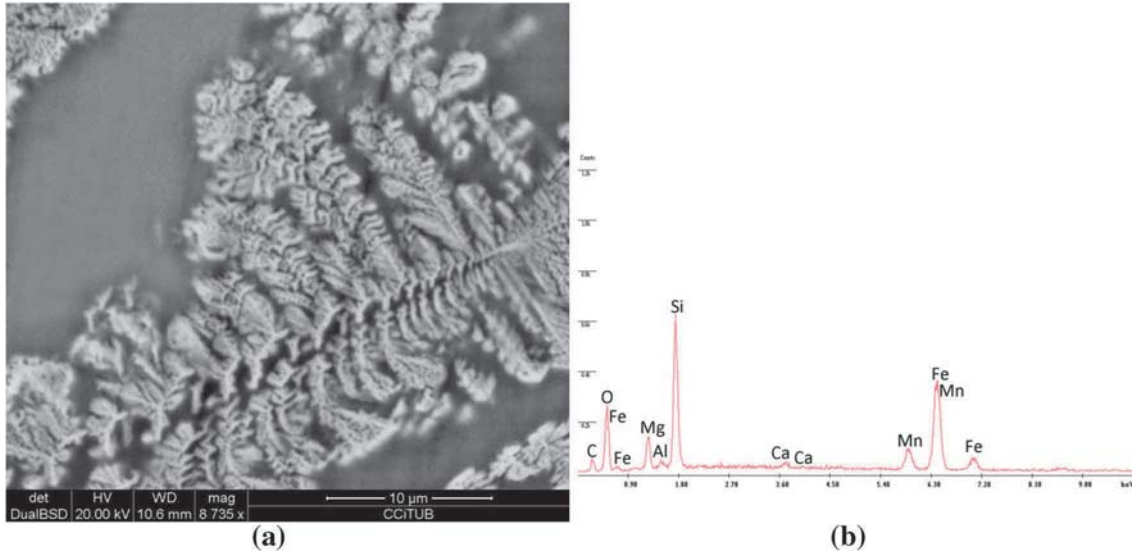


Figure 3. SEM micrograph showing the crystalline growth of a compound mainly composed by Si and O in the FR001 sample (a) and EDS microanalysis spectrum of the phase observed in the micrograph (b).

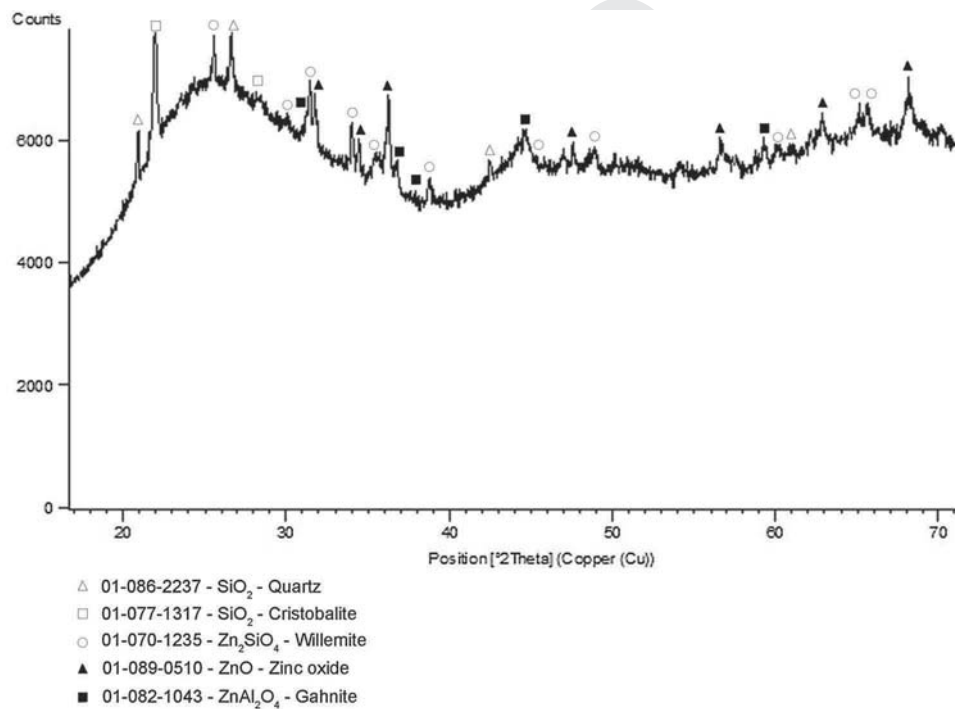


Figure 4. XRD diffractogram of the SC45F slag sample: ZnO, Zn₂SiO₄ and ZnAl₂O₄ compounds were found in addition to quartz and cristobalite.

411 that was stuck to the refractory lining is shown in
 412 Figure 6b. Regarding the refractory material, both a free-
 413 slag region and a darker region of a sample were analyzed
 414 by SEM–EDS. Only the expected peaks of silicon and
 415 oxygen were found for the free-slag region. However,
 416 detailed examinations on the darker region revealed the
 417 existence of slag penetrations¹⁰ similar to “veins” (indi-
 418 cated by arrows in Figure 7a where extra peaks of

419 aluminum, magnesium, calcium and cerium were detected
 420 in addition to the peaks of silicon and oxygen (see Fig-
 421 ure 7c). Most of these further elements found in the darker
 422 region are in good agreement with the use of standard
 423 metallic charges where returns become the main con-
 424 stituent (Table 2). Here it is worthy to emphasize the rel-
 425 evant intensity of the aluminum peak even though this
 426 element does not seem to be the most expectable one



Figure 5. General view of a discharged refractory lining still placed in an induction furnace. Mark 1 indicates the worn away level; mark 2 denotes the slags ring adhered to the refractory. Refractory lining is shown by the arrows.

427 according to the composition of the standard charges used
 428 here. In Figure 7b, a detailed view of a slag vein is also
 429 shown which is surrounded by SiO_2 grains. These slag
 430 penetrations in the refractory areas in contact with adhered
 431 slag probably make them darker.

432 Table 5 shows the chemical composition of the three slag
 433 samples that were collected from the discharged refractory
 434 linings. In this table, only the oxides with content higher
 435 than 1.00 wt% were included. Surprisingly, all three sam-
 436 ples are mainly composed by Al_2O_3 and MgO , while SiO_2
 437 becomes now a minority oxide when comparing to data
 438 include in Table 2. MgO and Al_2O_3 are two of the oxides
 439 included in Table 5 with the highest melting point, i.e.,

>2000 °C (3632 °F), so they should be more prone to be
 stuck to the refractory material than the rest of possible
 oxides. On the other hand, quartzite, i.e., the refractory
 material used in the present work, is essentially composed
 by SiO_2 which is considered as an acid oxide. Thus, one
 can expect that the basicity and the amphoteric charac-
 teristics of MgO and Al_2O_3 , respectively, also become a rel-
 evant cause of the reaction between these slags and the
 refractory material.

The available source of magnesium seems to be the foundry
 returns used as raw materials; however, the sources of
 aluminum are numerous. In this second case, possible
 supplies are the use of additives as ferrosilicon, silicon
 carbide, the use of steel scraps and also of foundry returns
 as raw materials. According to this fact and to the high
 Al_2O_3 content found in all the slag samples obtained from
 the refractory linings, it could be considered that aluminum
 plays a very relevant role on refractory degradations in
 electric furnaces and consequently on the life span reduc-
 tion in these devices. Table 5 also shows important
 amounts of cerium oxide and lanthanum oxide in these slag
 samples in comparison with those samples obtained
 directly from melts. The presence of these two elements
 should be related to the massive use of foundry returns as
 raw materials in the melting furnace. Notice that these
 returns are manufactured with the use of FeSiMg and of
 inoculants which both contain rare earth elements.

Figure 8 shows a SEM micrograph and the corresponding
 EDS microanalysis spectra obtained from four different
 constituents found in the UC11 sample. The microanalysis
 of the massive phase identified as 1 in this figure led to
 record peaks of aluminum, magnesium and oxygen in
 accordance with the results shown in Table 5. Notice that
 any peak of silicon was not detected in this compound.
 Another main phase (marked as 2) is composed by a group
 of elements (calcium, cerium, lanthanum, silicon, sulfur

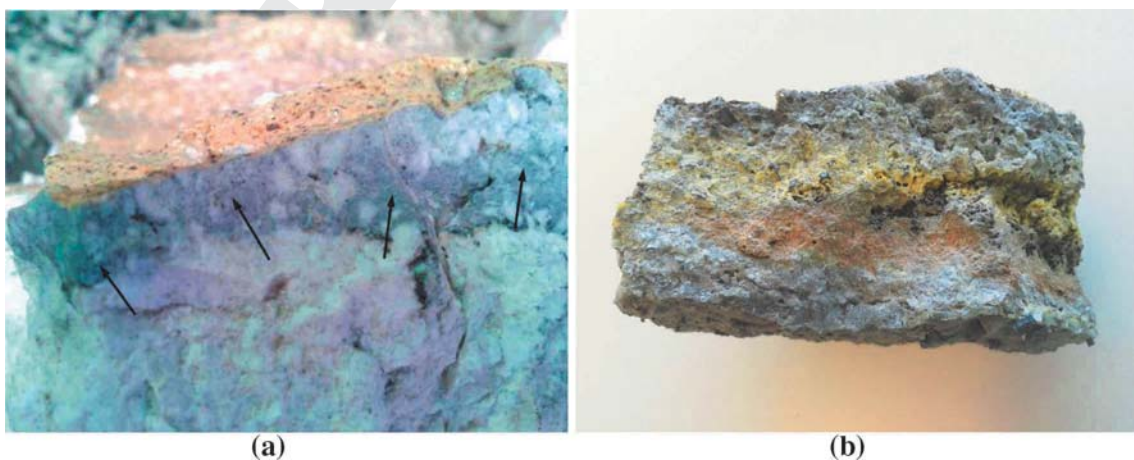


Figure 6. Detail of the darker areas found in the quartzite refractory lining in contact with slags (a); a general view of a typical slag adhered to the lining (b).

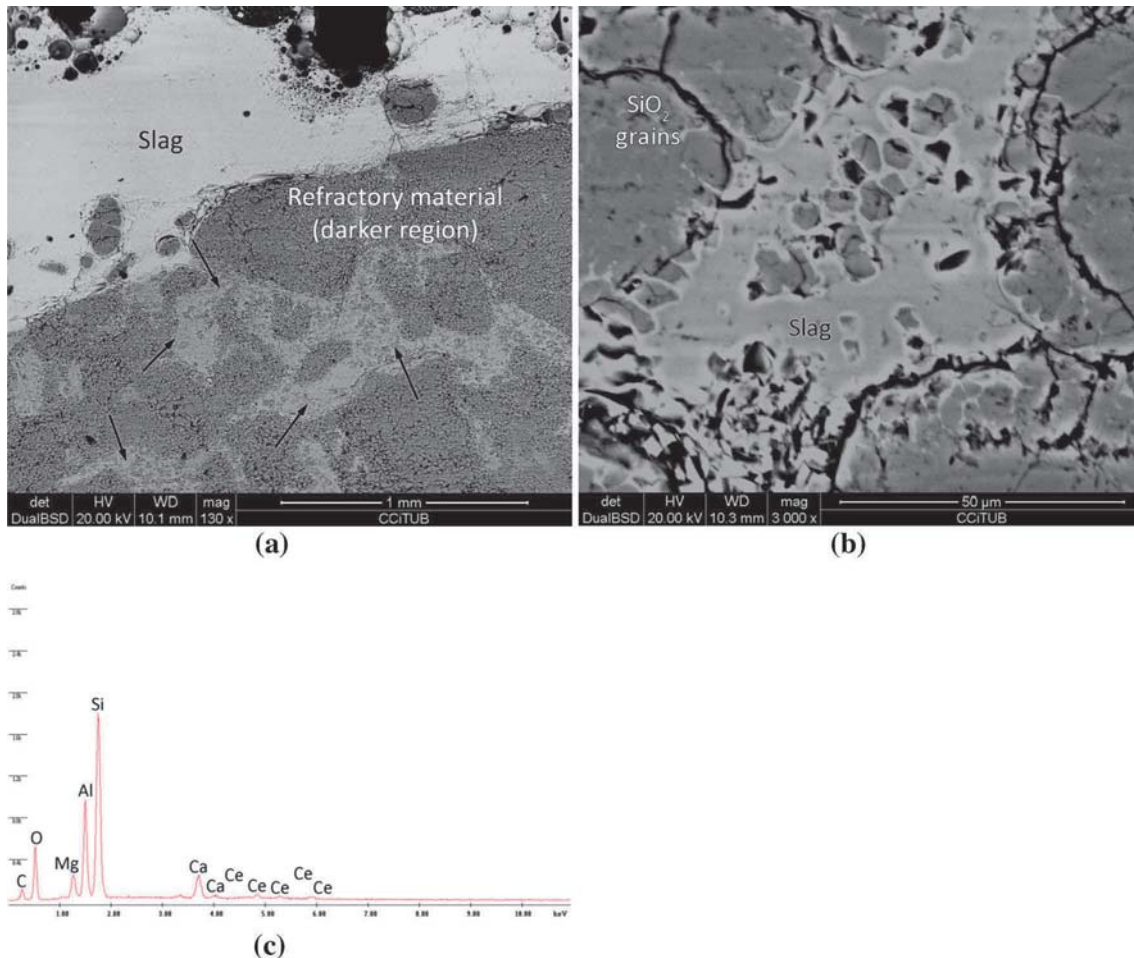


Figure 7. SEM micrographs of the refractory lining: Showing the slag (light zone) veins by arrows adhered to the darker region (refractory lining) (a); detail of the affected zone of the refractory (b); below the SEM-EDS spectrum of this affected zone is shown (c).

Table 5. Chemical Composition of Slags Stuck to the Refractory Lining Analyzed by XRF (wt%)

| Sample | Al ₂ O ₃ | MgO | SiO ₂ | CeO ₂ | Fe ₂ O ₃ | CaO | La ₂ O ₃ | SO ₃ |
|--------|--------------------------------|-------|------------------|------------------|--------------------------------|------|--------------------------------|-----------------|
| UC11 | 43.45 | 27.67 | 10.71 | 6.19 | 2.89 | 3.30 | 2.47 | 1.69 |
| UC31 | 61.81 | 24.95 | 5.86 | 2.87 | 1.72 | 1.37 | – | – |
| UC32 | 37.59 | 39.96 | 4.68 | 6.58 | 2.63 | 3.72 | 2.63 | 1.28 |

476 and oxygen) which can form complex sulfides and oxides.
 477 Finally, peaks of calcium and sulfur (likely to form CaS)
 478 are present in phase 4 which grew as isolated particles in
 479 phase 3, this latter composed by magnesium, silicon, calcium
 480 and oxygen.

481 The XRD diffractogram shown in Figure 9 was obtained
 482 from the UC32 slag sample. It can be seen that it contains a
 483 much smaller amount of amorphous phases than the slag
 484 samples obtained from the melts surface (see Figure 4).
 485 The UC11 and UC31 samples exhibit a similar behavior.
 486 This high crystalline degree must be related to the observed

heavy aspect of these slags when comparing to the floating
 ones.

The most important crystalline phase found in the UC32
 sample is the MgAl₂O₄ (spinel) which is formed by
 reaction between the two main oxides MgO and Al₂O₃
 present in these slags (Table 5). This result confirms the
 relevant role of aluminum previously predicted in the
 SEM inspections carried out on the slag-affected regions
 of refractory (Figure 7). On the other hand, this phase
 has been also detected in the SEM analysis of the UC11
 slag sample shown in Figure 8 (phase 1). The crystalline

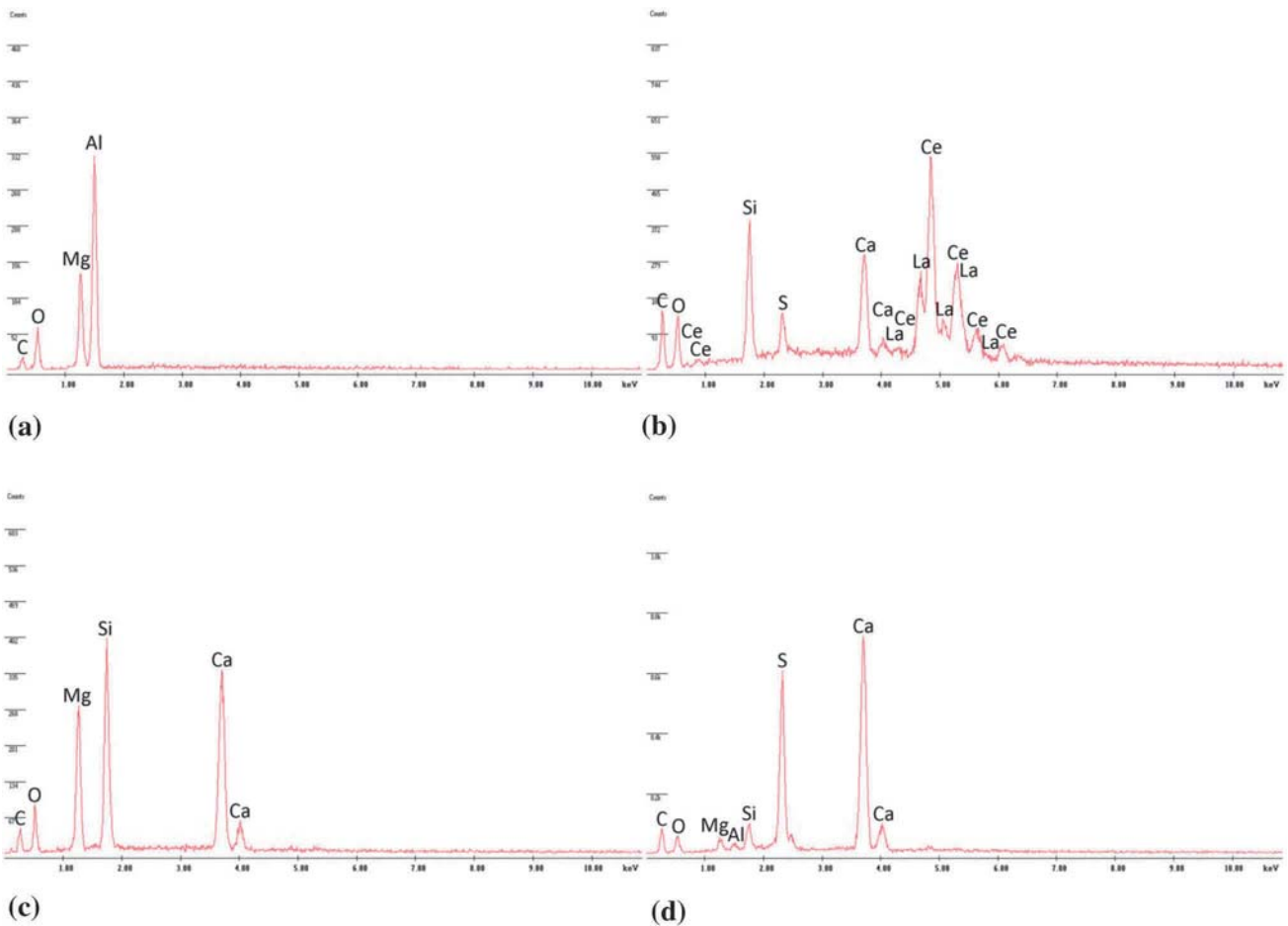
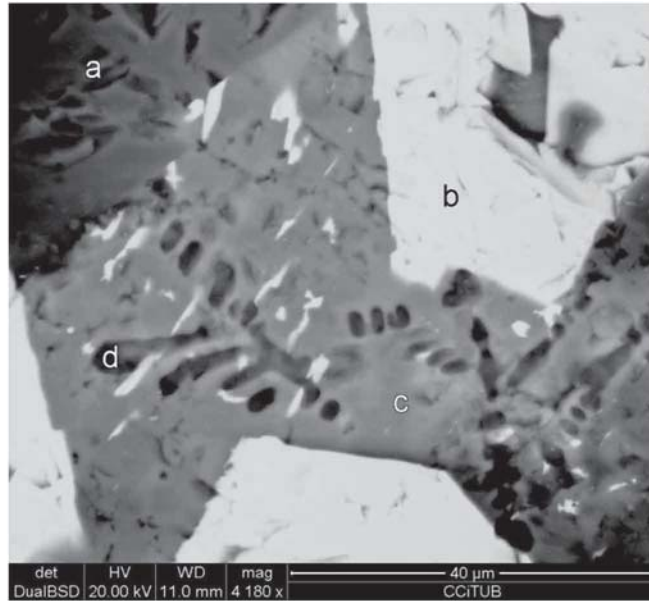


Figure 8. SEM micrograph of the UC11 slag sample (top). Below the EDS microanalysis spectra of the phases marked on micrograph are shown.

498 phase MgO (periclase) is also detected in the XRD indexation shown in Figure 9. This fact indicates that an excess
 499 of MgO which has not reacted with the Al₂O₃ to form the spinel is present in the UC32 sample. In fact, this sample
 500
 501

showed the highest MgO content (Table 5). Other minor phases identified in Figure 9 are CaMgSiO₄ (monticellite) and SiO₂ (quartz). The former compound has been also
 502
 503
 504
 505

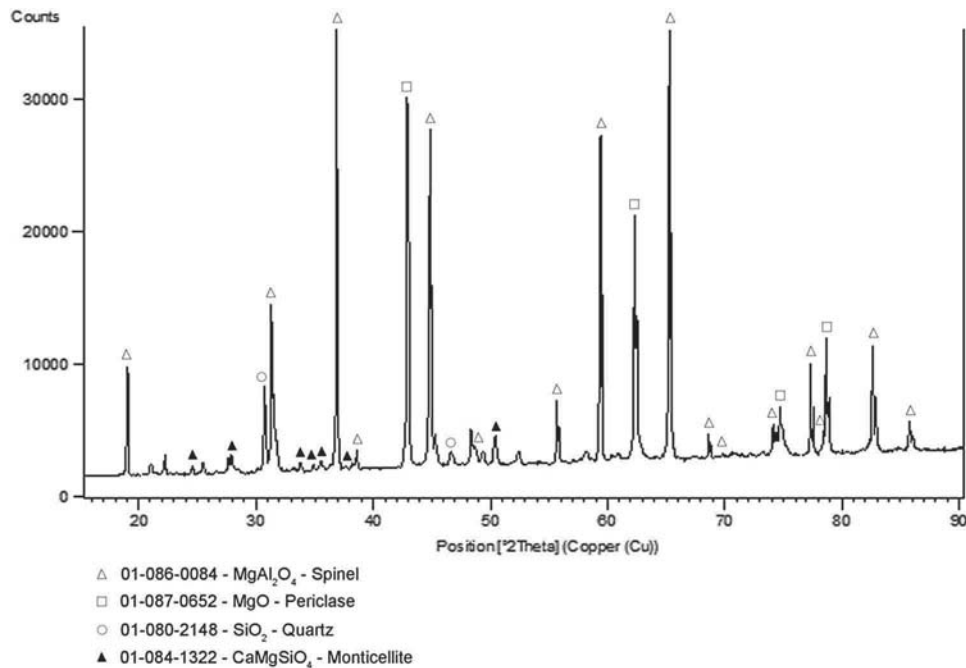


Figure 9. XRD diffractogram of the UC32 slag sample adhered to the refractory lining.

506 Comparing to the results obtained for the UC32 sample, the
 507 XRD characterization of UC11 and UC31 samples also
 508 showed a high crystalline degree, MgAl₂O₄ (spinel) was
 509 detected as the main crystalline phase and CaMgSiO₄
 510 (monticellite) and (Mg,Fe)₂SiO₄ (forsterite) were identified
 511 as minor phases. It is worth nothing that CaMgSiO₄ and
 512 CaS compounds had been already detected as phase 3 and
 513 phase 4, respectively, in the SEM-ESD analysis performed
 514 on the UC11 sample (Figure 8). The (Mg,Fe)₂SiO₄ (for-
 515 sterite) compound which is formed by the reaction between
 516 MgO and SiO₂ is only present in the UC11 slag sample as
 517 is shown the highest SiO₂ content (Table 5).

518 *Origin of Slags Adhered to Refractory Linings*

519 Once identified the spinel phase MgAl₂O₄ as the main con-
 520 stituent of slags adhered to refractory materials, it is now
 521 worthy to investigate the origin of this phase and some of its
 522 influencing factors. As it has been described in the experi-
 523 mental section, two different metallic charge compositions
 524 (mainly composed by foundry returns or by steel scrap) were
 525 separately used during the whole life span of each refractory
 526 lining of the furnace following a similar melting procedure.
 527 Malfunctions owing to the presence of slag stuck to the
 528 refractory lining were detected after 214 melting batches
 529 when steel scrap-based charges were only used in the melting
 530 furnace. However, no failure occurred after 724 melting
 531 batches when exclusively using the return-based charges.

532 Another important difference is the amount of slags
 533 adhered to the refractory linings at the end of their life

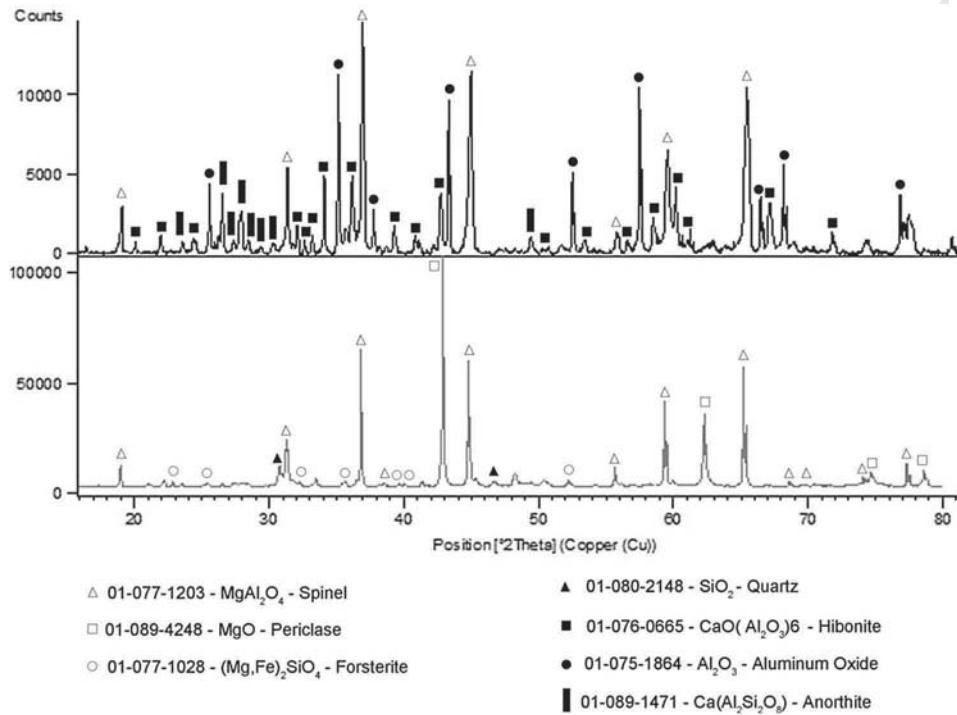
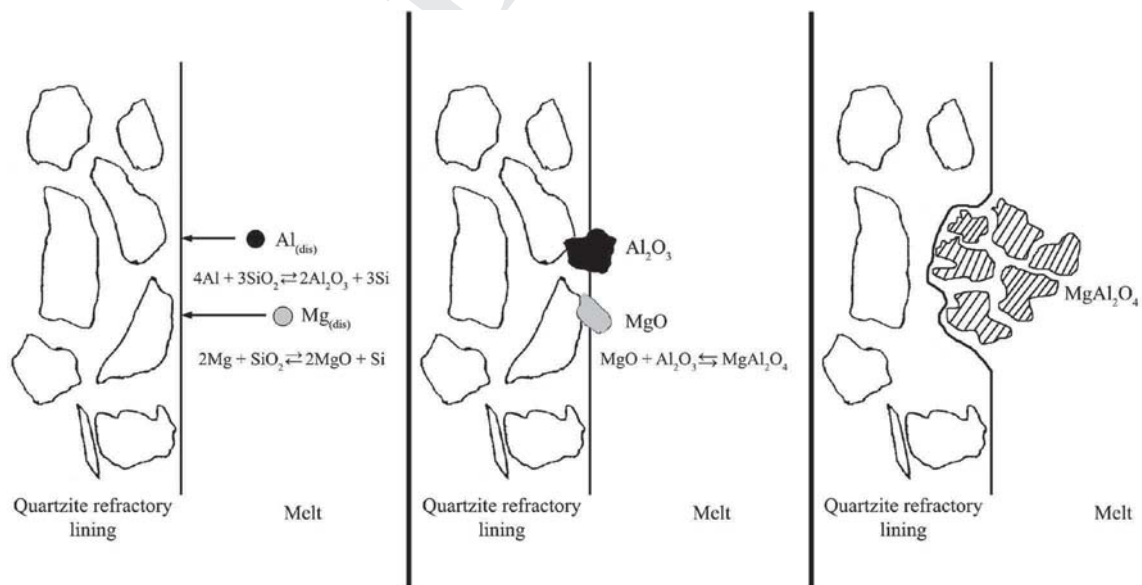
span. The lining where only steel scrap-based charges were
 used for melting shows massive slags stuck to the entire
 refractory ring located in the usual region described above.
 However, only specific zones of the lining were found to be
 affected when return-based charges were exclusively used
 following a similar melting procedure. Thus, it can be
 concluded that slag formation was more “aggressive” in
 the first case, based on the use of steel scrap-based charges.

XRF chemical compositions of the two slag samples
 collected from the linings are shown in Table 6 where
 only those contents higher than 1.00 wt% are included. It
 can be seen that the MgO, CeO₂ and La₂O₃ contents are
 higher for the sample obtained from the return-based
 charges than for the one coming from the steel scrap-
 based charges. On the contrary, the Al₂O₃ content is
 much lower in the FR21 sample than in the SC31 sample.
 These results are expected as foundry returns become a
 notorious source of the three elements previously men-
 tioned (they were manufactured using a FeSiMg alloy and
 inoculant), while steel scrap and the adjusting products
 (SiC and FeSi) contain significant amounts of aluminum.
 These auxiliary products should also be considered as the
 source of Ca and Zn in case of the slag sample formed in
 steel scrap-based melts.

Regarding the phases identified by XRD for these two slag
 samples, the spinel MgAl₂O₄ is the most abundant crys-
 talline phase on the FR21 sample (see the diffractogram
 shown in Figure 10 below). Additionally, an important
 amount of MgO (periclase) has been also found in this
 sample. The crystalline phases detected on the SC31

Table 6. Slag Samples Composition Analyzed by XRF (wt%)

| Sample | Al ₂ O ₃ | MgO | SiO ₂ | CeO ₂ | Fe ₂ O ₃ | CaO | La ₂ O ₃ | SO ₃ | ZnO |
|--------|--------------------------------|-------|------------------|------------------|--------------------------------|------|--------------------------------|-----------------|------|
| FR21 | 30.17 | 36.56 | 8.69 | 9.29 | 2.79 | 4.29 | 3.78 | 2.15 | – |
| SC31 | 60.61 | 7.48 | 16.66 | 1.16 | 4.60 | 6.28 | – | – | 1.13 |


Figure 10. XRD diffractogram and indexation of: the SC31 sample (above) and the FR21 sample (below).

Figure 11. Schema of the steps proposed for the adhered slags formation in the quartzite refractory linings.

564 sample are quite different (Figure 10 above). In this case,
 565 many phases that contain aluminum and calcium have been
 566 found, being the most relevant the $MgAl_2O_4$ spinel, Al_2O_3
 567 (corundum), $CaAl_2Si_2O_8$ (anorthite) and an aluminum–
 568 calcium oxide known as hibonite. These XRD outcomes
 569 are in good agreement with the differences shown in
 570 Table 6, all confirming the negative effect of aluminum on
 571 life span of refractory linings.

572 A scheme that illustrates the mechanism and the probable
 573 reactions involved in the formation of slags adhered to the
 574 refractory linings is shown in Figure 11. Part of the alu-
 575 minium dissolved in the melt would react with the quartzite
 576 giving aluminum oxide and silicon as final products.
 577 Similarly, the magnesium dissolved can react with the
 578 refractory material to obtain magnesium oxide and silicon.
 579 Thus, these two oxides would be present close to the lining,
 580 so they can react to form the spinel ($MgAl_2O_4$) previously
 581 characterized as the mainly phase of these detrimental slag
 582 compounds.

583 Additional experiments were made using different melting
 584 furnaces in order to evaluate the detrimental effect of
 585 aluminum coming from FeSi and SiC products. Thus,
 586 apparently favorable metallic charges composed 58 %
 587 foundry returns, 37 % steel scrap, 2.5 % pig iron, 1.7 %
 588 graphite and 0.8 % FeSi with a low aluminum content
 589 (0.029 wt%) and without any SiC addition were exclu-
 590 sively used during the whole life span of 22 refractory
 591 linings. As a result of these experiments, it was observed
 592 that slags were adhered to 20 discharged refractory linings,
 593 whereas they were not found in the other 2 ones. When SiC
 594 was reintroduced again to metallic charges according to the
 595 standard composition of charges (Table 2), both the per-
 596 centage of affected linings and the amount of slags adhered
 597 to them slightly increased. These results show the impor-
 598 tant role of steel scrap as the main aluminum source of
 599 melts prepared in the present work.

600 Conclusions

601 Characterization of the slag samples analyzed in the present
 602 work has led to know both the chemical and structural
 603 differences between slags formed in the upper surface of
 604 melts and those adhered to the refractory lining of medium
 605 frequency induction furnaces. In this second case, serious
 606 malfunctions are normally detected on these devices which
 607 force to stop the melting process and finally to replace the
 608 refractory lining with important extra costs for foundry
 609 plants. The main conclusions of this work are the following:

610 1. Slags floating in melt surfaces contain high
 611 amounts of amorphous constituents probably
 612 due to their rapid formation. This fact could
 613 explain the vitreous aspect normally found on
 614 these slags at room temperature. The majority

615 crystalline phases detected on these floating slags
 616 are SiO_2 as quartz and cristobalite. The rest of
 617 compounds (oxides) detected by XRF and not
 618 identifiable by XRD techniques are included in
 619 the amorphous fraction of this slags.

2. In general, significant differences have not been
 620 detected regarding chemical composition and
 621 constituent phases between the slag samples
 622 collected just after finishing the melting of
 623 metallic charges and the corresponding ones
 624 obtained after remaining melts in contact with
 625 open air for 45 min. In this sense, only an
 626 increase in some oxides as Al_2O_3 was found in
 627 case of samples from steel scrap-based charges.
 628
3. Floating slags formed when using steel scrap-
 629 based charges showed the highest zinc and
 630 aluminum contents and they are the only samples
 631 where a crystalline phase ($ZnAl_2O_4$, gahnite)
 632 different than SiO_2 was detected by XRD tech-
 633 niques. These high zinc and aluminum contents
 634 are due to the use of galvanized steel scrap as raw
 635 material (Zn and potentially Al) and of FeSi and
 636 SiC as additives (Al). On the other hand, rests of
 637 nondissolved additives as FeSi, SiC and graphite
 638 have been also detected on these samples.
 639
4. In case of slags formed from return-based charges,
 640 zinc and aluminum contents are low, while the
 641 content of those elements involved in the manu-
 642 facture of ductile iron castings (Mg, Ce and La)
 643 becomes comparatively high. The XRD analyses
 644 made on these slags revealed the existence of
 645 minor amounts of silicates that contain these
 646 specific elements in addition to the SiO_2 phase.
 647
5. Slags attached to the quartzite refractory lining of
 648 the induction furnaces and considered as the more
 649 detrimental ones mainly consist of $MgAl_2O_4$
 650 (spinel) which is probably formed by reaction
 651 between Al_2O_3 and MgO compounds.
 652
6. Slags adhered to the refractory lining show
 653 chemical compositions quite different from those
 654 found in floating ones. In the former case, Al_2O_3
 655 and MgO become the most abundant oxides on
 656 the samples analyzed and their content depends
 657 on the metallic charge composition and on the
 658 amount and type of additives used during the
 659 melting procedure. It has been demonstrated in
 660 the present study that the highest amount of slags
 661 stuck to the refractory material were found when
 662 a high content of Al_2O_3 is present in the slag
 663 composition. Thus, aluminum must play a critical
 664 role in the detrimental effect of these slags on the
 665 life span of refractory linings.
 666
7. It has been checked that those adhered slags with a
 667 high Al_2O_3 content and considered more “aggres-
 668 sive” against quartzite linings are promoted when
 669 using steel scrap-based metallic charges during
 670 melting. This result leads to think that steel scrap
 671



672 is the most important available source of alu-
673 minum though SiC and FeSi products have also to
674 be taken into account regarding this sense.
675 8. Finally, it has been possible to minimize the
676 formation of slags adhered to linings by reducing
677 the aluminum sources in raw materials and additives
678 used in the melting processes. An effective control
679 to keep a proper balance among MgO, SiO₂ and
680 Al₂O₃ oxides during melting should be quite helpful
681 to prevent the formation of the MgAl₂O₄ spinel
682 phase and consequently of these harmful slags.

683 Acknowledgments

684 This work has been financially supported by Fundería
685 Condals S.A foundry and by Catalan Government by
686 awarding the scholarship from AGAUR for the Indus-
687 trial PhD. The authors would like to acknowledge
688 scientific and technological centers (CCiT) from the
689 University of Barcelona for the collaboration in all the
690 analysis.

REFERENCES

- | | |
|--|-----|
| 1. P.R. Khan, W.M. Su, H.S. Kim, J.W. Kang, J.F. Wallace, AFS Trans. 172 , 105–116 (1987) | 692 |
| 2. M. Gagné, M.-P. Paquin, P.-M. Cabanne, FTJ, 276–280 (2009) | 693 |
| 3. ITP Metal casting, BCS, Incorporated (November 2005) | 694 |
| 4. Vivek R. Gandhewar, Satish V. Bansod, Atul B. Borade, IJET 3 (4), 277–284 (2011) | 695 |
| 5. A. Loizaga, J. Sertucha, R. Suárez, Rev Metal Madrid 44 (5), 432–446 (2008) | 696 |
| 6. R.W. Heine, C.R. Loper, MOD CAST, 50 (3), 155-122 (1966) | 697 |
| 7. C. Labrecque, M. Gagné, E. Planque, <i>Keith Millis Symposium on Ductile Cast Iron</i> (2003) | 698 |
| 8. S. Katz, AFS Trans., Paper 04-132(05), 2–13 (2004) | 699 |
| 9. Peter J. Heaney, Rev. Mineral. Geochem. 29 , 1–40 (1994) | 700 |
| 10. W.E. Lee, S. Zhang, Int. Mater. Rev. 44 (3), 77–104 (1999) | 701 |

691

692

693

694

695

696

697

698

699

700

701

702

703

704

705

706

707

708

709

710

Journal : **40962**

Article : **25**



Author Query Form

Please ensure you fill out your response to the queries raised below and return this form along with your corrections

Dear Author

During the process of typesetting your article, the following queries have arisen. Please check your typeset proof carefully against the queries listed below and mark the necessary changes either directly on the proof/online grid or in the 'Author's response' area provided below

| Query | Details Required | Author's Response |
|-------|---|-------------------|
| AQ1 | Figures 2, 4, 8, 9, 10 are poor in quality as it looks fuzzy. Please supply a high-resolution version of the said figure preferably in .tiff or .jpeg format with 300 dpi resolution. | |
| AQ2 | Please provide volume number for reference [2]. | |